MINISTRY OF EDUCATION AND TRAINING
HO CHI MINH CITY UNIVERSITY OF TECHNOLOGY AND ENGINEERING

NGUYEN VAN TOAN

PROPOSING AND EVALUATING PERFORMANCE OF HYBRID SATELLITE–TERRESTRIAL RELAY NETWORK USING FOUNTAIN CODES

Major: Electronic Engineering
Major code: 9520203

SUMMARY OF PH.D. THESIS

HO CHI MINH CITY – 2026

This thesis was completed at

HCMC University of Technology and Engineering

Supervisor 1: Assoc. Prof. Dr. Pham Ngoc Son
Supervisor 2: Assoc. Prof. Dr. Tran Trung Duy

The dissertation will be defended before the Departmental (Faculty-Level) Dissertation Evaluation Committee convened at Ho Chi Minh City University of Technology and Engineering on , 2026.

INTRODUCTION

Research Motivation

The rapid growth of data traffic in modern wireless communication systems, together with smart devices, the Internet of Things (IoT), and digital services, is imposing increasingly stringent requirements on communication networks, including high data rates, low latency, massive connectivity, and high reliability. Although terrestrial mobile networks have achieved significant advancements over successive generations, their ability to meet these requirements remains limited in wide-area coverage scenarios or under unfavorable conditions such as maritime regions, mountainous areas, and infrastructure-deficient zones.

In this context, the integration of satellite and terrestrial networks, particularly hybrid satellite–terrestrial relay networks (HSTRNs), has emerged as an effective solution to extend coverage and enhance reliability. However, HSTRNs still face challenges such as severe path loss, deep fading, and co-channel interference, which degrade transmission performance. Under such conditions, fixed-rate coding techniques cannot effectively adapt to channel variations.

Fountain codes (FC), with their rateless property and flexible packet accumulation capability, are a promising solution to improve reliability in harsh environments. In addition, advanced techniques such as non-orthogonal multiple access (NOMA), partial relay selection (PRS), and reconfigurable intelligent surfaces (RIS) have been shown to enhance spectral efficiency, diversity gain, and channel quality.

However, existing HSTRN studies mainly consider these techniques independently and do not incorporate FC, particularly from the perspective of physical layer security and in the presence of co-channel interference. Therefore, investigating HSTRN models integrating FC with advanced techniques is necessary to simultaneously improve reliability and security.

Motivated by these issues, the topic: **"Proposing and Evaluating Performance of Hybrid Satellite–Terrestrial Relay Network Using Fountain Codes"** is of significant importance, with clear scientific and practical relevance in next-generation wireless systems. The results of this dissertation contribute to the theoretical foundation for analyzing HSTRN performance under complex channel conditions and provide important design guidelines to enhance reliability and physical layer security in practical deployments.

Contributions of the Dissertation

First, an HSTRN model employing fountain codes in the presence of co-channel interference (CCI) is proposed. Closed-form expressions for outage probability (OP) and system outage probability (SOP) are derived and verified via Monte-Carlo simulations for both conventional (ConV) and proposed (ProP) schemes. Results show that ProP effectively exploits the packet accumulation mechanism of fountain codes, significantly improving reliability and reducing CCI impact compared to ConV. In addition, a joint optimization of power allocation and transmission time is addressed, demonstrating optimal parameter configurations and providing design guidelines for HSTRNs under adverse conditions.

Second, the dissertation develops a multi-cluster PLS–NOMA–HSTRN model integrating fountain codes and partial relay selection (PRS) with multiple eavesdroppers. Analytical expressions for OP, IP, SOP, and SIP are derived and validated. Results indicate that the proposed model improves both reliability and security while clarifying their trade-off and identifying optimal parameters, particularly the power allocation coefficient.

Third, a PLS–HSTRN model integrating RIS with NOMA, fountain codes, and PRS is proposed, and analytical expressions for OP, SOP, IP, and SIP are derived. Results show that RIS significantly enhances channel quality and system performance through reflection gain and spatial diversity. Furthermore, the dissertation clarifies the trade-off among reliability, security, and latency, and determines optimal parameter regions for system design. These findings provide a foundation for developing and optimizing multi-technology HSTRNs in next-generation wireless networks.

In general, the dissertation results strengthen the theoretical foundation and provide effective design guidelines for multi-technology HSTRN systems in next-generation wireless communication networks.

Chapter 1: Overview

In recent years, HSTRNs have been considered a promising solution to extend coverage and enhance reliability for advanced 5G and 6G systems. Meanwhile, FC provides channel adaptability and packet loss resilience, whereas NOMA, PRS, and RIS improve spectral efficiency, diversity gain, and channel quality. However, existing studies mainly investigate these techniques independently, while the integration of FC into multi-technology HSTRNs remains limited. In particular, the impact of CCI on the packet accumulation

mechanism of FC, as well as the role of FC in the trade-off between reliability and security when combined with NOMA, PRS, and RIS, has not been thoroughly studied. Therefore, developing HSTRN models that integrate FC with advanced techniques is necessary to effectively exploit technological potential and improve both system performance and PLS.

Chapter 2: Theoretical Background

Chapter 2 presents the theoretical foundations of HSTRN systems, including system models and channel characteristics of satellite–terrestrial and terrestrial–terrestrial links under fading models such as Shadowed–Rician, Rayleigh, and Nakagami-m. In addition, this chapter introduces the principles and packet accumulation mechanism of FC, along with NOMA and RIS techniques, thereby clarifying their capability to enhance reliability, spectral efficiency, and channel quality. These contents provide the foundation for system modeling and performance and security analysis in the subsequent chapters.

Chapter 3: HSTRN Systems Using FC in the Presence of CCI

3.1. Introduction

The content of Chapter 3 is developed based on the results reported:

$[\mathrm{C}_1]$. N. V. Toan, T. T. Duy, P. N. Son, D. T. Hung, N. Q. Sang and T. L. Thanh, "Outage Performance Of Hybrid Satellite-Terrestrial Relaying Networks With Rateless Codes In Co-Channel Interference Environment," in *2023 ICSSE*, Ho Chi Minh, Vietnam, pp. 468–473, Jul. 2023.

3.2. System Model

The HSTRN–FC system is considered in the presence of Q CCI sources, where the satellite S transmits data to U_n via R. The packets p_{S} are transmitted using the DF protocol; at R, at least $G_{\min}$ packets are required for successful decoding, with a maximum of $H_{\max}$ transmissions; all nodes are equipped with a single antenna. The system consists of two schemes. In the conventional scheme (ConV), R performs DF on a per-packet basis without storage, where transmission occurs over two hops $\mathrm{S} \to \mathrm{R}$ and $\mathrm{R} \to \mathrm{U}_n$ under the impact of CCI, depending on the time allocation factor τ_{ConV}. In the proposed scheme (ProP), R is equipped with a buffer to accumulate FC packets: the first time slot is identical to that of ConV; the second time slot includes two cases: (i) if $G_{\min}$ has not been reached, R simultaneously stores and forwards packets; (ii) if $G_{\min}$ is satisfied, R performs decoding and proactively transmits FC packets to U_n, without relying on the time allocation between the two slots.

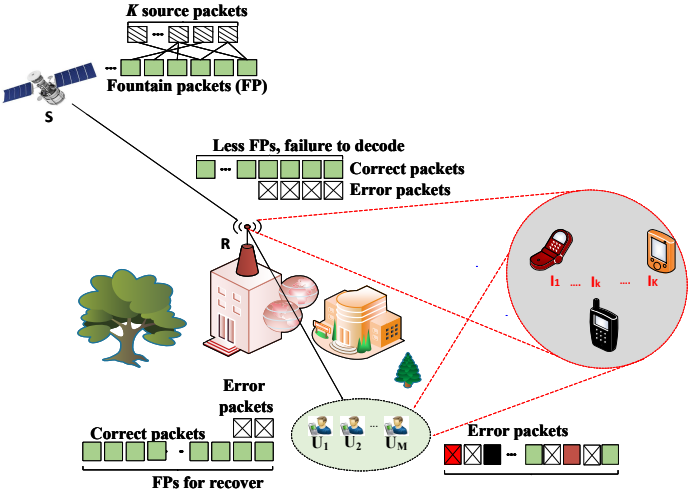

Fig.3.1: HSTRN system model using FC under the impact of CCI.

3.3. Performance Analysis

3.3.1. Successful Decoding Probability of an FC Packet

This section presents the derivation of closed-form expressions for the successful decoding probability of an FC packet for both ConV and ProP.

3.3.2. Outage Probability of Users

The OP of U_n for the two schemes is determined by (1) and (2).

$$\mathrm{OP}_n^{\mathrm{ConV}} = \sum_{L_n^{\mathrm{ConV}}=0}^{G_{\min}-1} \binom{H_{\max}}{L_n^{\mathrm{ConV}}} \left(\theta_{\mathrm{U}_n}^{\mathrm{ConV}}\right)^{L_n^{\mathrm{ConV}}} \left(1-\theta_{\mathrm{U}_n}^{\mathrm{ConV}}\right)^{H_{\max}-L_n^{\mathrm{ConV}}}. \quad (1)$$

3.3.3. System Outage Probability In this section, the system outage probability (SOP) is analyzed, from which exact closed-form expressions are derived for both the ConV and ProP schemes, as presented in (3) and (4). Based on these analytical results, the impact of key system parameters, including NOMA, FC, and CCI, on the SOP is characterized.

$$\mathrm{OP}_n^{\mathrm{ProP}} = 1 - \sum_{T_{\mathrm{S}}=G_{\min}}^{H_{\max}} \left\{ \begin{array}{l} \binom{T_{\mathrm{S}}-1}{G_{\min}-1} \left(\theta_{\mathrm{SR}}^{\mathrm{ProP}}\right)^{G_{\min}} \left(1-\theta_{\mathrm{SR}}^{\mathrm{ProP}}\right)^{T_{\mathrm{S}}-G_{\min}} \\ \times \sum\limits_{L_{n,\mathrm{Case\,1}}^{\mathrm{ProP}}=0}^{G_{\min}} \sum\limits_{\substack{L_{n,\mathrm{Case\,2}}^{\mathrm{ProP}}=0 \\ L_{n,\mathrm{Case\,1}}^{\mathrm{ProP}}+L_{n,\mathrm{Case\,2}}^{\mathrm{ProP}} \geq G_{\min}}}^{H_{\max}-T_{\mathrm{S}}} \\ \times \binom{G_{\min}}{L_{n,\mathrm{Case\,1}}^{\mathrm{ProP}}} \left(\theta_{\mathrm{RU}_n}^{\mathrm{ProP,Case\,1}}\right)^{L_{n,\mathrm{Case\,1}}^{\mathrm{ProP}}} \\ \times \left(1-\theta_{\mathrm{RU}_n}^{\mathrm{ProP,Case\,1}}\right)^{G_{\min}-L_{n,\mathrm{Case\,1}}^{\mathrm{ProP}}} \binom{H_{\max}-T_{\mathrm{S}}}{L_{n,\mathrm{Case\,2}}^{\mathrm{ProP}}} \\ \times \left(\theta_{\mathrm{RU}_n}^{\mathrm{ProP,Case\,2}}\right)^{L_{n,\mathrm{Case\,2}}^{\mathrm{ProP}}} \left(1-\theta_{\mathrm{RU}_n}^{\mathrm{ProP,Case\,2}}\right)^{H_{\max}-T_{\mathrm{S}}-L_{n,\mathrm{Case\,2}}^{\mathrm{ProP}}} \end{array} \right\}. \tag{2}$$

$$\mathrm{SOP}_{\mathrm{ConV}} = 1 - \sum_{L_{\mathrm{R}}^{\mathrm{ConV}}=G_{\min}}^{H_{\max}} \left\{ \begin{array}{l} \binom{H_{\max}}{L_{\mathrm{R}}^{\mathrm{ConV}}} \left(\theta_{\mathrm{SR}}^{\mathrm{ConV}}\right)^{L_{\mathrm{R}}^{\mathrm{ConV}}} \left(1-\theta_{\mathrm{SR}}^{\mathrm{ConV}}\right)^{H_{\max}-L_{\mathrm{R}}^{\mathrm{ConV}}} \\ \times \prod\limits_{n=1}^{N} \left[\begin{array}{l} \sum\limits_{L_n^{\mathrm{ConV}}=G_{\min}}^{L_{\mathrm{R}}^{\mathrm{ConV}}} \binom{L_{\mathrm{R}}^{\mathrm{ConV}}}{L_n^{\mathrm{ConV}}} \left(\theta_{\mathrm{RU}_n}^{\mathrm{ConV}}\right)^{L_n^{\mathrm{ConV}}} \\ \times \left(1-\theta_{\mathrm{RU}_n}^{\mathrm{ConV}}\right)^{L_{\mathrm{R}}^{\mathrm{ConV}}-L_n^{\mathrm{ConV}}} \end{array} \right] \end{array} \right\}. \tag{3}$$

$$\mathrm{SOP}_{\mathrm{ProP}} = 1 - \sum_{T_{\mathrm{S}}=G_{\min}}^{H_{\max}} \left\{ \begin{array}{l} \binom{T_{\mathrm{S}}-1}{G_{\min}-1} \left(\theta_{\mathrm{SR}}^{\mathrm{ProP}}\right)^{G_{\min}} \left(1-\theta_{\mathrm{SR}}^{\mathrm{ProP}}\right)^{T_{\mathrm{S}}-G_{\min}} \\ \times \prod\limits_{n=1}^{N} \left[\begin{array}{l} \sum\limits_{L_{n,\mathrm{Case\,1}}^{\mathrm{ProP}}=0}^{G_{\min}} \binom{G_{\min}}{L_{n,\mathrm{Case\,1}}^{\mathrm{ProP}}} \left(\theta_{\mathrm{RU}_n}^{\mathrm{ProP,Case\,1}}\right)^{L_{n,\mathrm{Case\,1}}^{\mathrm{ProP}}} \\ \times \left(1-\theta_{\mathrm{RU}_n}^{\mathrm{ProP,Case\,1}}\right)^{G_{\min}-L_{n,\mathrm{Case\,1}}^{\mathrm{ProP}}} \\ \times \sum\limits_{\substack{L_{n,\mathrm{Case\,2}}^{\mathrm{ProP}}=0 \\ L_{n,\mathrm{Case\,1}}^{\mathrm{ProP}}+L_{n,\mathrm{Case\,2}}^{\mathrm{ProP}} \geq G_{\min}}}^{H_{\max}-T_{\mathrm{S}}} \binom{H_{\max}-T_{\mathrm{S}}}{L_{n,\mathrm{Case\,2}}^{\mathrm{ProP}}} \\ \times \left(\theta_{\mathrm{RU}_n}^{\mathrm{ProP,Case\,2}}\right)^{L_{n,\mathrm{Case\,2}}^{\mathrm{ProP}}} \left(1-\theta_{\mathrm{RU}_n}^{\mathrm{ProP,Case\,2}}\right)^{H_{\max}-T_{\mathrm{S}}-L_{n,\mathrm{Case\,2}}^{\mathrm{ProP}}} \end{array} \right] \end{array} \right\}. \tag{4}$$

3.3.4. Joint Power and Time Allocation Problem

The joint power and time allocation optimization problem is defined in (5) and detailed in Algorithms 1, 2, and 3.

$$\min_{\substack{0<\tau_X<1\\0<\mu_X<1}} \text{SOP}_X. \tag{5}$$

3.4. Simulation Results and Discussion

This section presents simulation results to validate the analysis and evaluate the impact of parameters on OP and SOP for the ConV and ProP schemes, while identifying optimal configurations.

The results in Fig. 3.2 presents that OP saturates at high SNR, confirming CCI as the limiting factor. Increasing $H_{\max}$ significantly improves reliability (up to 95% in some scenarios), while ProP outperforms ConV due to FC packet accumulation, at the cost of higher latency..

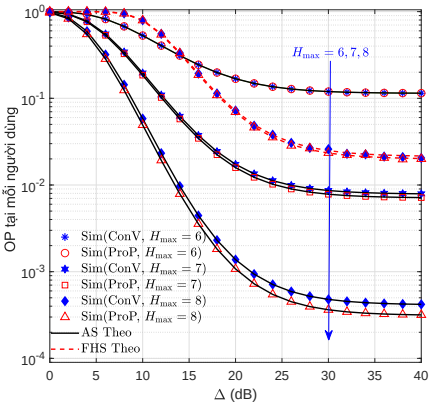

Fig. 3.2: OP at U_n versus Δ (dB) with $\mu_{\text{ConV}} = \mu_{\text{ProP}} = 0.5$ and $\tau_{\text{ConV}} = \tau_{\text{ProP}} = 0.5$.

Fig. 3.3 illustrates that OP strongly depends on τ_X, and an optimal τ_X exists for each μ_X to minimize OP. Near-optimal performance is achieved at $\mu_X \approx 0.5$, reflecting a balanced power allocation between the two hops.

Fig. 3.4 show that SOP decreases with Δ and saturates at high SNR due to CCI. The ProP scheme achieves lower SOP than ConV, while SOP increases with the number of users N due to higher OP.

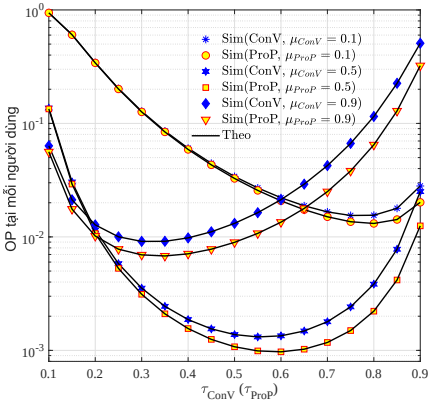

Fig.3.3: OP at U_n versus τ_{ConV}, τ_{ProP} with $\Delta = 20$ dB and $H_{\max} = 8$.

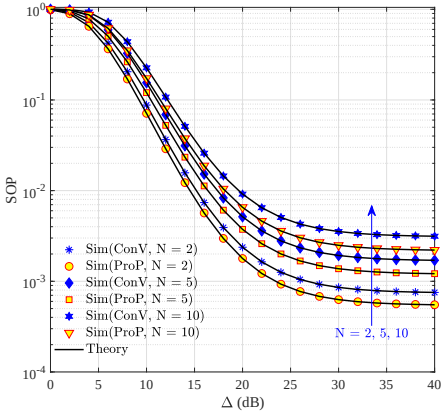

Fig. 3.4: SOP versus Δ (dB) with $\mu_{\text{ConV}} = \mu_{\text{ProP}} = 0.5$, $\tau_{\text{ConV}} = \tau_{\text{ProP}} = 0.5$.

The results in Fig. 3.5 reveals that SOP decreases as $H_{\max}$ increases, and an optimal τ_X exists to minimize SOP. The ProP scheme outperforms the conventional scheme, confirming the effectiveness of the packet accumulation mechanism in enhancing security.

Fig. 3.6 presents SOP strongly depends on μ_X, with an optimal μ_X for each scheme. Combined with Fig. 3.5, this indicates joint power and time optimization is necessary for optimal performance.

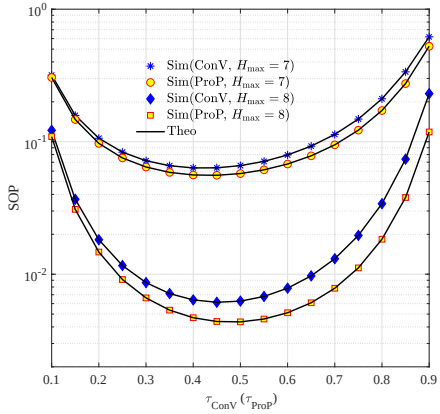

Fig. 3.5: SOP versus τ_{ConV} (τ_{ProP}) with $\Delta = 20$ dB, $\mu_{\text{ConV}} = \mu_{\text{ProP}} = 0.65$, and $N = 5$.

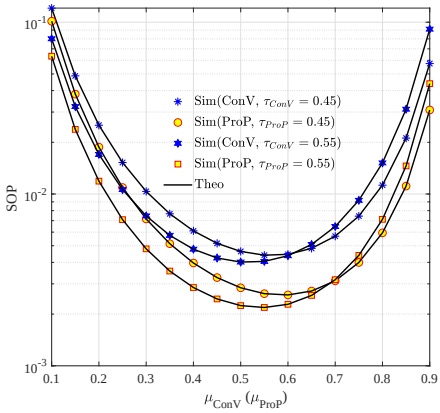

Fig. 3.6: SOP versus μ_{ConV} and μ_{ProP} with $\Delta = 15$ dB, $N = 8$, and $H_{\max} = 9$.

Fig. 3.7 illustrates that SOP decreases significantly with optimal (μ_X, τ_X), especially at high Δ and $H_{\max}$. The performance gap between ProP and ConV widens as $H_{\max}$ increases, indicating that combining resource optimization with FC packet accumulation improves performance and enlarges the gain over the conventional scheme.

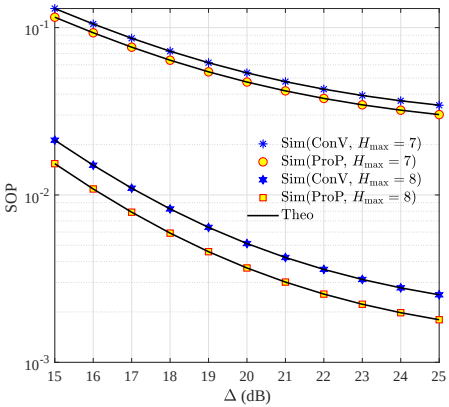

Fig. 3.7: SOP versus Δ (dB) with optimal (μ_X, τ_X) for $N = 5$.

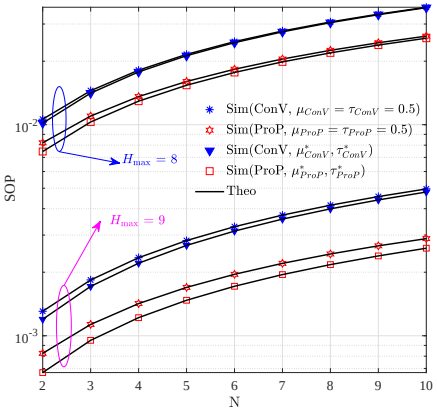

Fig. 3.8: SOP versus the number of users N with $\Delta = 15$ dB.

Fig. 3.8 shows that SOP increases with the number of users N, while increasing $H_{\max}$ significantly improves performance. The ProP scheme consistently outperforms ConV, and performance improves with larger $H_{\max}$, confirming that the packet accumulation mechanism is key to maintaining performance in multi-user scenarios.

3.5. Conclusion

Chapter 3 proposes and analyzes an HSTRN model using FC under

CCI, where packet accumulation at the relay improves reliability. Closed-form expressions for OP and SOP of the ConV and ProP schemes are derived and validated via simulations, showing performance is limited by CCI at high SNR, while ProP outperforms due to packet accumulation, achieving SOP reductions of 20%–50% and OP reductions up to 95% as $H_{\max}$ increases, at the cost of higher latency. The resource optimization problem confirms optimal (μ, τ), highlighting the importance of resource allocation. However, the model does not consider multi-user scenarios and advanced security, which will be addressed in the next chapter through NOMA and relay selection.

Chapter 4: NOMA–HSTRN Systems Using Fountain Codes and PRS

4.1. Introduction

The content of Chapter 4 is reported in J_1 and C_2.

[J_1]. N. V. Toan, T. T. Duy, P. N. Son, P. V. Tuan, and T. L. Thanh, "Security-Reliability analysis of NOMA-assisted hybrid satellite-terrestrial relay multicast transmission networks using Fountain codes and partial relay selection in the presence of multiple eavesdroppers," *EAI Endorsed Transactions on Industrial Networks and Intelligent Systems*, vol. 12, no. 3, Apr. 2025.

[C_2]. N. V. Toan, N. V. Hien, P. X. Minh, and P. N. Son, "Performance Evaluation of Hybrid Satellite–Terrestrial Relaying Broadcast Networks Using Fountain Codes and NOMA," in *Proc. IEEE Int. Conf. Consumer Electronics–Asia (ICCE-Asia)*, Danang, Vietnam, Jul. 2024, pp. 1–4.

4.2. System Model

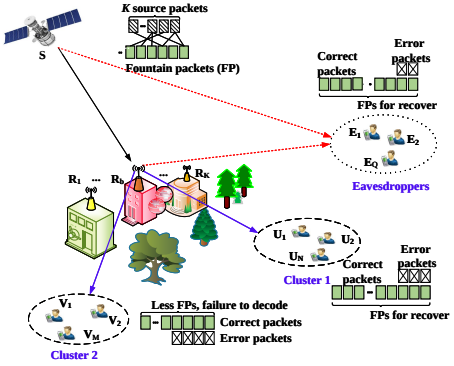

Fig. 4.1: HSTRN system model using FC.

The PLS–HSTRN system consists of a satellite S transmitting data to two user clusters U and V via K relays, as no direct links exist. A relay R_b is selected via PRS based on the best channel condition. The system includes Q eavesdroppers intercepting signals from S and R_b; thus, randomization and relaying strategies enhance security. All nodes use a single antenna and operate in half-duplex mode.

Based on the system model, the dissertation derives the received signal expressions at the user clusters and the eavesdropper group. From these, the SNR is obtained, forming the basis for analyzing system performance and physical layer security.

4.3. System Performance Analysis

4.3.1. Successful Decoding Probability of an FC Packet

Mathematical analysis is performed to derive closed-form expressions for the decoding probability of an FC packet in the cases described in Table 4.1.

4.3.2. System Reliability Analysis

$$\mathrm{OP}_{\mathrm{U}} = 1 - \sum_{r=G_{\min}}^{H_{\max}} \binom{H_{\max}}{r} (\theta_{\mathrm{R}_b,p_{\mathrm{V}},p_{\mathrm{U}}})^r (1-\theta_{\mathrm{R}_b,p_{\mathrm{V}},p_{\mathrm{U}}})^{H_{\max}-r} \times \left[\sum_{l=G_{\min}}^{r} C_r^l \chi_{\mathrm{U},p_{\mathrm{U}}}^l (1-\chi_{\mathrm{U},p_{\mathrm{U}}})^{r-l} \right]^N . \quad (6)$$

Table 4.1: Signal processing at R_b and E_q in two time slots

Receiving node	**First time slot**	**Second time slot**
R_b	**Case 1:** R_b successfully decodes both packets p_{V} and p_{U} from S	R_b re-encodes and forwards p_{V} and p_{U} to the two user clusters
	Case 2: R_b successfully decodes p_{V} but fails to decode p_{U}	R_b re-encodes and forwards only p_{V} to cluster V
E_q	**Case 3.1:** E_q successfully decodes both p_{V} and p_{U} from S	No decoding is performed in the second time slot
	Case 3.2: E_q decodes p_{V} but fails to decode p_{U}	E_q performs SIC, removes p_{V}, and decodes p_{U} from R_b
	Case 3.3: E_q decodes p_{V} from S	p_{V} is not decoded in the second time slot

$$\mathrm{OP_V} = 1 - \sum_{t_{\mathrm{tot}}=G_{\min}}^{H_{\max}} \sum_{t_1=0}^{t_{\mathrm{tot}}} \binom{H_{\max}}{t_1} \binom{H_{\max}-t_1}{t_{\mathrm{tot}}-t_1}$$
$$\times \ \left(\theta_{\mathrm{R}_b,p_{\mathrm{V}},p_{\mathrm{U}}}\right)^{t_1} \left(\theta_{\mathrm{R}_b,p_{\mathrm{V}},\overline{p_{\mathrm{U}}}}\right)^{t_{\mathrm{tot}}-t_1} \times \left(1-\theta_{\mathrm{R}_b,p_{\mathrm{V}},p_{\mathrm{U}}}-\theta_{\mathrm{R}_b,p_{\mathrm{V}},\overline{p_{\mathrm{U}}}}\right)^{H_{\max}-t_{\mathrm{tot}}}$$
$$\times \left[\begin{array}{c} \sum_{r_1=0}^{t_1} \sum_{r_2=0,\, r_1+r_2\geq G_{\min}}^{t_2} \binom{t_1}{r_1}\binom{t_2}{r_2} \left(\chi_{\mathrm{V},p_{\mathrm{V}}}\right)^{r_1} \left(1-\chi_{\mathrm{V},p_{\mathrm{V}}}\right)^{t_1-r_1} \\ \times \left(\tau_{\mathrm{V},p_{\mathrm{V}}}\right)^{r_2} \left(1-\tau_{\mathrm{V},p_{\mathrm{V}}}\right)^{t_2-r_2} \end{array} \right]^{M}. \quad (7)$$

$$\mathrm{SOP} = 1 - (1-\mathrm{OP_U}) \times (1-\mathrm{OP_V}). \quad (8)$$

4.3.3. System Security Analysis

$$\mathrm{IP}_{\mathrm{E}_q,p_i} = \sum_{r=G_{\min}}^{H_{\max}} \binom{H_{\max}}{r} \left(\Lambda_{\mathrm{E}_q,p_i}\right)^{r} \left(1-\Lambda_{\mathrm{E}_q,p_i}\right)^{H_{\max}-r}. \quad (9)$$

$$\mathrm{IP}_i = 1 - \prod_{q=1}^{Q} \left(1-\mathrm{IP}_{\mathrm{E}_q,p_i}\right) = 1 - \left(1-\mathrm{IP}_{\mathrm{E}_q,p_i}\right)^{Q}. \quad (10)$$

$$\mathrm{SIP} = \mathrm{IP_U} + \mathrm{IP_V} - \mathrm{IP_U} \times \mathrm{IP_V}. \quad (11)$$

4.4. Results and Discussion

This section presents simulation results to validate the analytical expressions and evaluate the impact of system parameters on the performance of the proposed model.

Fig. 4.2 illustrates that performance strongly depends on channel conditions, where the AS channel outperforms FHS (e.g., $\mathrm{OP_V}$ decreases from 4×10^{-1} to 2×10^{-3} at $\Delta = 16$ dB). Increasing $H_{\max}$ significantly improves performance in FHS (up to 93.3% reduction) due to FC packet accumulation, at the cost of higher latency. In addition, both $\mathrm{OP_U}$ and $\mathrm{OP_V}$ decrease with Δ, with $\mathrm{OP_U}$ dropping faster at high SNR due to SIC efficiency.

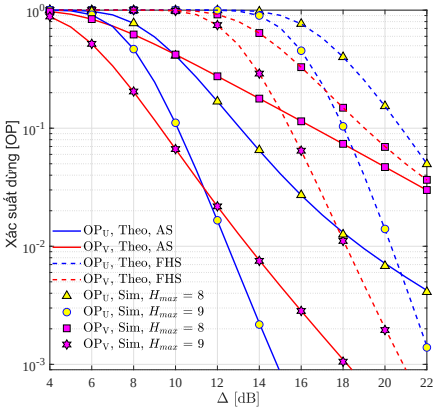

Fig. 4.2: OP of the clusters versus Δ (dB) with $G_{\min} = 8$ and $\alpha_U = 0.25$.

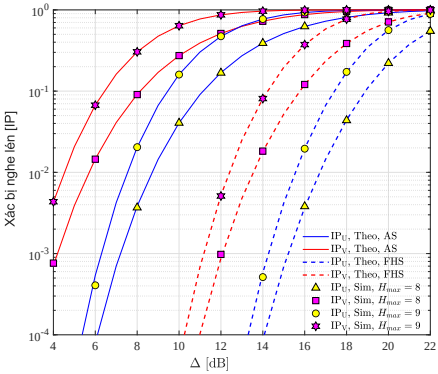

Fig. 4.3: IP of the clusters versus Δ (dB) with $G_{\min} = 8$ and $\alpha_U = 0.25$.

Fig. 4.3 presents that IP_U and IP_V increase with $H_{\max}$ (e.g., at $\Delta = 18$ dB, IP_U increases fivefold as $H_{\max}$ rises from 8 to 9) due to more FC packets increasing the decoding capability of eavesdroppers. Meanwhile, IP_i increases with Δ and is higher in AS than in FHS. Combined with Fig. 4.2, this clearly illustrates the trade-off between OP and IP.

Fig. 4.4 shows that OP_U and OP_V vary inversely with α_U due to NOMA constraints and decrease significantly as K increases due to PRS; for example,

OP_{U} drops by over two orders of magnitude as K increases from 1 to 5 at $\alpha_{\mathrm{U}} = 0.25$. In addition, the balance point between the two clusters shifts as K increases, highlighting the role of power allocation in reliability balancing.

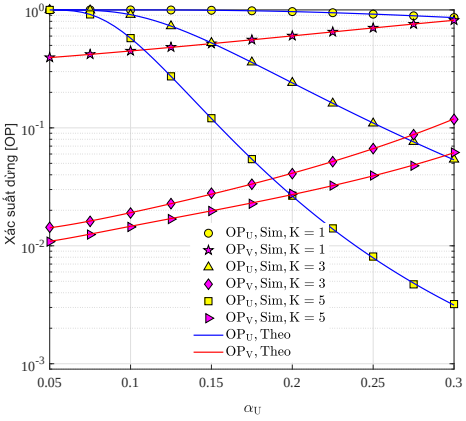

Fig. 4.4: OP of the clusters versus α_{U} with $\Delta = 10$ dB, $G_{\min} = 8$, and $H_{\max} = 9$.

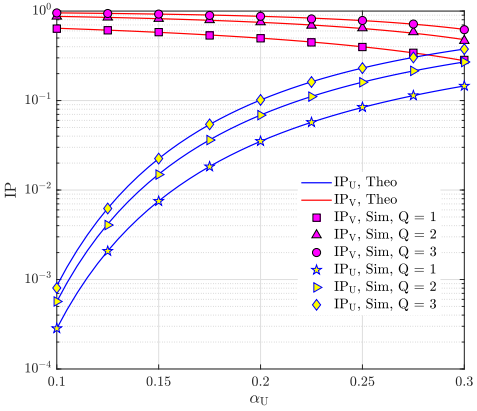

Fig. 4.5: IP of the clusters versus α_{U} with $\Delta = 10$ dB, $G_{\min} = 8$, and $H_{\max} = 9$.

Fig. 4.5 indicates that IP increases with the number of eavesdroppers Q due to improved FC packet collection capability. Meanwhile, $\mathrm{IP_U}$ increases with α_{U}, while $\mathrm{IP_V}$ slightly decreases, reflecting the NOMA power allocation mechanism. Therefore, selecting an appropriate α_{U} can control the eavesdropping level between clusters.

Fig. 4.6 reveals that SOP decreases rapidly with Δ, indicating improved reliability. For $\alpha_{\mathrm{U}} = 0.1$, SOP is higher at low Δ but drops sharply and becomes lower at high Δ due to the dominance of $\mathrm{OP_U}$ in (8), whereas $\alpha_{\mathrm{U}} = 0.3$ yields a smoother decline. Hence, proper selection of α_{U} and Δ enables effective SOP control.

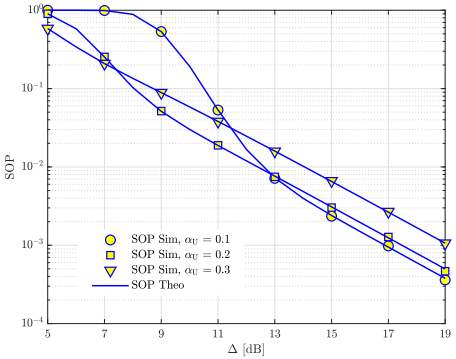

Fig. 4.6: SOP versus Δ with $G_{\min} = 8$ and $H_{\max} = 9$.

Fig. 4.7 demonstrates that SIP increases with Δ due to improved interception capability of eavesdroppers. Notably, at low Δ, selecting $\alpha_{\mathrm{U}} = 0.3$ reduces SIP, thereby enhancing security performance.

Fig. 4.8 indicates that SOP decreases significantly as K increases due to the diversity gain of PRS; for example, at $\alpha_{\mathrm{U}} = 0.2$, SOP drops from 6×10^{-1} to 1×10^{-2} as K increases from 3 to 10 (about 60-fold). In addition, an optimal α_{U} exists to minimize SOP, shifting with K. The results also suggest that system performance can be optimized through joint design of power allocation and the number of relays K.

4.5. Chapter 4 Conclusion

Chapter 4 proposes and analyzes a multi-cluster PLS–NOMA–HSTRN model integrating NOMA, PRS, and FC in the presence of multiple eaves-

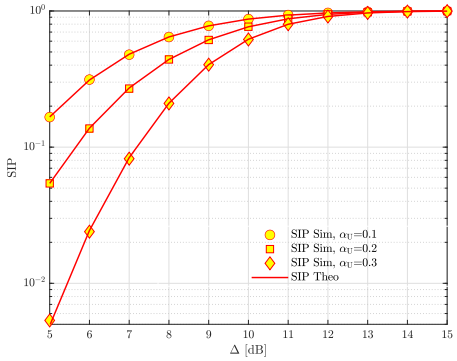

Fig. 4.7: SIP versus Δ with $G_{\text{min}} = 8$ and $H_{\text{max}} = 9$.

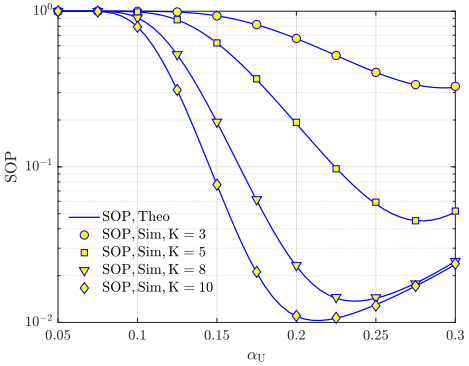

Fig. 4.8: SOP versus α_{U} with $\Delta = 7.5$ dB, $G_{\text{min}} = 8$, and $H_{\text{max}} = 10$.

droppers, thereby significantly improving reliability and security. Closed-form expressions for OP, IP, SOP, and SIP are derived and validated via simulations, showing close agreement. Results indicate that increasing K and H_{max} reduces OP and SOP, but increases IP and SIP, highlighting the trade-off between reliability and security. In addition, optimal parameter configurations, particularly α_{U} and H_{max}, enable performance balancing among clusters and system optimization. Overall, the results confirm the effectiveness of the proposed model and provide a foundation for extension to advanced architectures.

Chapter 5: NOMA–HSTRN Systems Using FC and RIS

5.1. Introduction

The content of Chapter 5 is reported in J_2:

[J_2]. N. V. Toan, P. N. Son, T. T. Duy, T. L. Thanh, and T. V. Thanh, "Performance evaluation of hybrid satellite–terrestrial relay networks using fountain codes, NOMA, and RIS," *REV Journal on Electronics and Communications*, vol. 15, no. 3, Jul.–Sep. 2025. DOI: 10.21553/rev-jec.415.

5.2. System Model

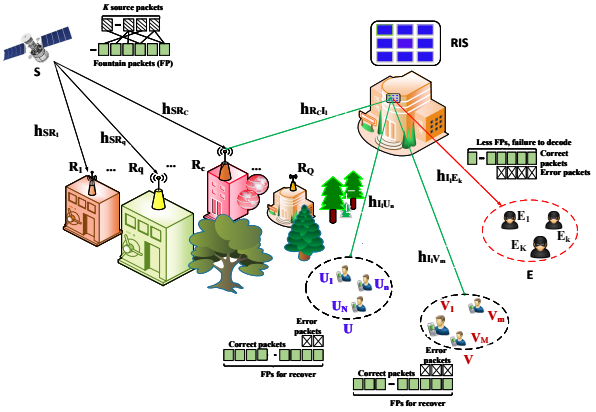

Fig.5.1: System Model.

Fig. 5.1 illustrates the proposed PLS–HSTRN model, where the satellite S transmits signals to ground user clusters via a combination of FC and NOMA. To support transmission, the system employs K DF relays with PRS, along with an RIS of L elements to enhance channel quality, mitigate interference, and improve security. The reflected signals are delivered to two user clusters: the near cluster U (N users) and the far cluster V (M users). The system also considers Q eavesdroppers. All nodes are equipped with a single antenna, half-duplex mode, and transmission occurs over two time slots.

5.2.1. Channel Model

This section presents the satellite–terrestrial and terrestrial–terrestrial channel models for system analysis.

5.2.2. Signal Model

The received signal model and SNR expressions of the proposed RIS-assisted system are established for the two time slots, while two benchmark models, namely AF and WoRIS, are also developed for reliability and security performance comparison.

5.3. System Performance Analysis

5.3.1. Successful Decoding Probability of an FC Packet

This section derives the expressions for the successful decoding probability of FC packets at the ground receiving nodes.

5.3.2. Outage Probability of Clusters and System

$$\mathrm{OP_U} = 1 - \sum_{r=G_{\min}}^{H_{\max}} \binom{H_{\max}}{r} \left(\theta_{\mathrm{R}_b}^{p_\mathrm{V},p_\mathrm{U}}\right)^r \left(1-\theta_{\mathrm{R}_b}^{p_\mathrm{V},p_\mathrm{U}}\right)^{H_{\max}-r} \times \left[\sum_{p=G_{\min}}^{r} \binom{r}{p} \left(\chi_{\mathrm{U}_n}^{p_\mathrm{U}}\right)^p \left(1-\chi_{\mathrm{U}_n}^{p_\mathrm{U}}\right)^{r-p}\right]^N . \tag{12}$$

$$\mathrm{OP_V} = 1 - \sum_{t_{\mathrm{tot}}=G_{\min}}^{H_{\max}} \sum_{t_1=0}^{t_{\mathrm{tot}}} \left[\begin{array}{l} \times \binom{H_{\max}}{t_1} \binom{H_{\max}-t_1}{t_{\mathrm{tot}}-t_1} \left(\theta_{\mathrm{R}_b}^{p_\mathrm{V},p_\mathrm{U}}\right)^{t_1} \\ \times \left(\theta_{\mathrm{R}_b}^{p_\mathrm{V},\overline{p_\mathrm{U}}}\right)^{t_{\mathrm{tot}}-t_1} \left(1-\theta_{\mathrm{R}_b}^{p_\mathrm{V},p_\mathrm{U}}-\theta_{\mathrm{R}_b}^{p_\mathrm{V},\overline{p_\mathrm{U}}}\right)^{H_{\max}-t_{\mathrm{tot}}} \end{array} \right] \times \left[\begin{array}{l} \times \sum_{r_1=0}^{t_1} \sum_{\substack{r_2=0 \\ r_1+r_2 \geq G_{\min}}}^{t_2} \binom{t_1}{r_1} \binom{t_2}{r_2} \left(\chi_{\mathrm{V}_m}^{p_\mathrm{V}}\right)^{r_1} \left(1-\chi_{\mathrm{V}_m}^{p_\mathrm{V}}\right)^{t_1-r_1} \\ \times \left(\tau_{\mathrm{V}_m}^{p_\mathrm{V}}\right)^{r_2} \left(1-\tau_{\mathrm{V}_m}^{p_\mathrm{V}}\right)^{t_2-r_2} \end{array} \right]^M . \tag{13}$$

SOP is defined as the probability that at least one of the two clusters experiences outage:

$$\mathrm{SOP} = 1 - \left(1-\mathrm{OP_U}\right)\left(1-\mathrm{OP_V}\right). \tag{14}$$

5.3.3. Intercept Probability of Clusters and System

Using analytical methods and based on Table 5.1, the intercept probability is derived as follows.

Table 5.1. Successful interception scenarios of fountain-coded packets

FC packet	R_b	E_q
p_{U}	$\gamma_{\mathrm{S,R}_b}^{p_{\mathrm{V}}} > \gamma_{\mathrm{R}}^{th},\ \gamma_{\mathrm{S,R}_b}^{p_{\mathrm{U}}} > \gamma_{\mathrm{R}}^{th}$	$\gamma_{\mathrm{R}_b,\mathrm{E}_q}^{p_{\mathrm{V}}} > \gamma_{\mathrm{E}}^{th},\ \gamma_{\mathrm{R}_b,\mathrm{E}_q}^{p_{\mathrm{U}}} > \gamma_{\mathrm{E}}^{th}$
p_{V}	**Case 1:** $\gamma_{\mathrm{S,R}_b}^{p_{\mathrm{V}}} > \gamma_{\mathrm{R}}^{th},\ \gamma_{\mathrm{S,R}_b}^{p_{\mathrm{U}}} > \gamma_{\mathrm{R}}^{th}$	$\gamma_{\mathrm{R}_b,\mathrm{E}_q}^{p_{\mathrm{V}}} > \gamma_{\mathrm{E}}^{th}$
	Case 2: $\gamma_{\mathrm{S,R}_b}^{p_{\mathrm{V}}} > \gamma_{\mathrm{R}}^{th},\ \gamma_{\mathrm{S,R}_b}^{p_{\mathrm{U}}} \le \gamma_{\mathrm{R}}^{th}$	$\psi_{\mathrm{R}_b\mathrm{E}_q}^{p_{\mathrm{V}}} > \gamma_{\mathrm{E}}^{th}$

$$\mathrm{IP_U} = \sum_{r=G_{\min}}^{H_{\max}} \binom{H_{\max}}{r} \left(\theta_{\mathrm{R}_b}^{p_{\mathrm{V}},p_{\mathrm{U}}}\right)^r \left(1-\theta_{\mathrm{R}_b}^{p_{\mathrm{V}},p_{\mathrm{U}}}\right)^{H_{\max}-r} \times \left\{1-\left[\sum_{p=G_{\min}}^{r}\binom{r}{p}\left(\chi_{\mathrm{E}_q}^{p_{\mathrm{U}}}\right)^p\left(1-\chi_{\mathrm{E}_q}^{p_{\mathrm{U}}}\right)^{r-p}\right]^Q\right\}. \tag{15}$$

$$\mathrm{IP_V} = \left[\begin{array}{l} \times \sum_{t_{\mathrm{tot}}=G_{\min}}^{H_{\max}} \sum_{t_1=0}^{t_{\mathrm{tot}}} \binom{H_{\max}}{t_1}\binom{H_{\max}-t_1}{t_{\mathrm{tot}}-t_1}\left(\theta_{\mathrm{R}_b}^{p_{\mathrm{V}},p_{\mathrm{U}}}\right)^{t_1} \\ \times \left(\theta_{\mathrm{R}_b}^{p_{\mathrm{V}},\overline{p_{\mathrm{U}}}}\right)^{t_{\mathrm{tot}}-t_1}\left(1-\theta_{\mathrm{R}_b}^{p_{\mathrm{V}},p_{\mathrm{U}}}-\theta_{\mathrm{R}_b}^{p_{\mathrm{V}},\overline{p_{\mathrm{U}}}}\right)^{H_{\max}-t_{\mathrm{tot}}} \end{array}\right] \times \left\{1-\left[\begin{array}{l} \times \sum_{r_1=0}^{t_1}\sum_{\substack{r_2=0 \\ r_1+r_2\ge G_{\min}}}^{t_2}\binom{t_1}{r_1}\binom{t_2}{r_2}\left(\chi_{\mathrm{E}_q}^{p_{\mathrm{V}}}\right)^{r_1}\left(1-\chi_{\mathrm{E}_q}^{p_{\mathrm{V}}}\right)^{t_1-r_1} \\ \times \left(\tau_{\mathrm{E}_q}^{p_{\mathrm{V}}}\right)^{r_2}\left(1-\tau_{\mathrm{E}_q}^{p_{\mathrm{V}}}\right)^{t_2-r_2} \end{array}\right]^Q\right\}. \tag{16}$$

The system intercept probability (SIP) is defined as

$$\mathrm{SIP} = 1-(1-\mathrm{IP_U})(1-\mathrm{IP_V}). \tag{17}$$

5.4. Results and Discussion

This section presents simulation results evaluating system performance in terms of OP, IP, SOP, and SIP, and compares with benchmark models to highlight advantages and trade-offs.

Fig. 5.2 indicates that OP decreases while IP increases as Δ or L grows,

reflecting the reliability–security trade-off; for sufficiently large L, RIS provides gains comparable to diversity, enabling the system to outperform benchmark models, but requires proper tuning of L for performance balance.

Fig. 5.3 presents that increasing $H_{\max}$ significantly improves reliability (OP) but degrades security (IP), leading to a three-way trade-off among latency, reliability, and security.

Results from Fig. 5.4 indicates that SOP and SIP exhibit a clear system-level trade-off; the proposed model achieves an optimal balance by tuning L and α_{U}, offering greater flexibility than benchmark models.

Fig. 5.5 indicates that α_{U} and K strongly affect reliability; PRS combined with RIS significantly improves performance, and an optimal balance point exists between clusters.

Results from Fig. 5.6 demonstrates that the number of eavesdroppers Q increases IP and SIP, with SIP dominated by the cluster with higher IP; tuning α_{U} enables balancing security levels between clusters.

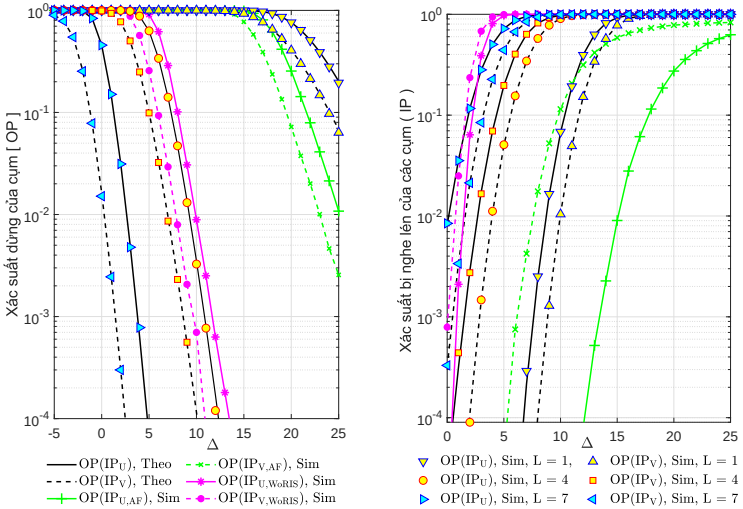

(a) OP (b) IP

Fig. 5.2: OP and IP versus Δ (dB) with L, $G_{\min} = 4$, $H_{\max} = 6$, and $\alpha_{\mathrm{U}} = 0.25$.

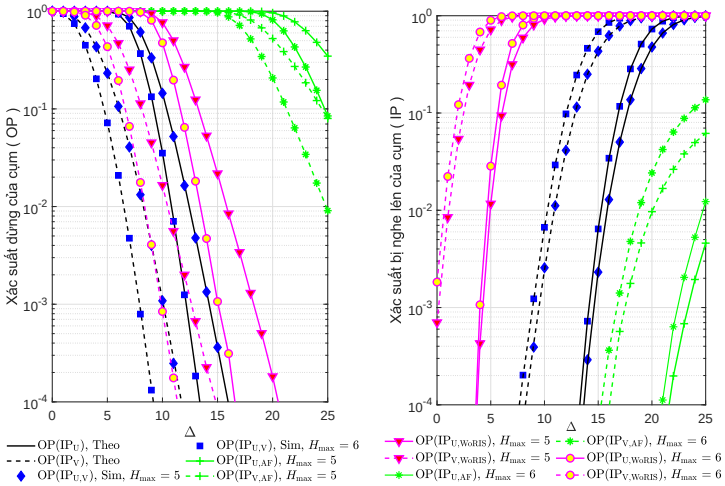

(a) OP (b) IP

Fig. 5.3: OP and IP versus Δ (dB) with $H_{\max}$, $G_{\min} = 4$, $L = 4$, and $\alpha_{\mathrm{U}} = 0.2$.

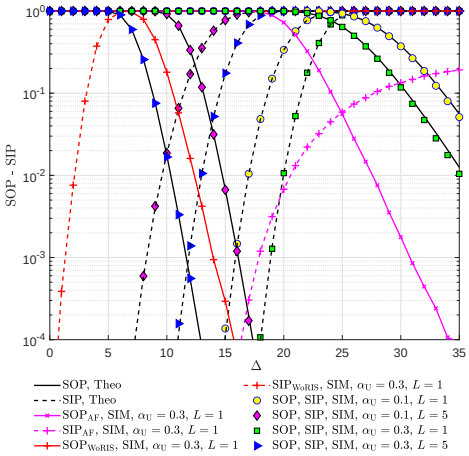

Fig. 5.4: SOP and SIP versus Δ (dB) with α_{U}, L, $H_{\max} = 6$, and $G_{\min} = 4$.

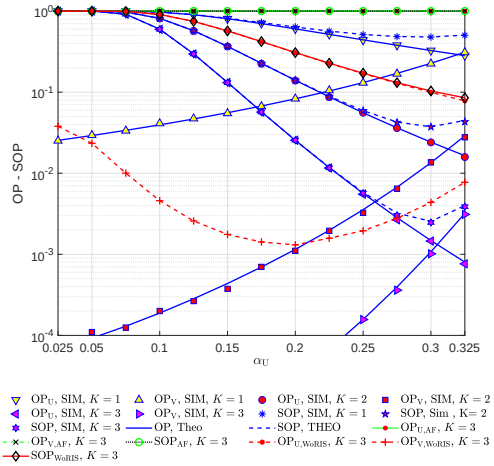

Hình 5.5: SOP versus α_U with $\Delta = 10$ dB, $L = 4$, $G_{\min} = 4$, and $H_{\max} = 6$.

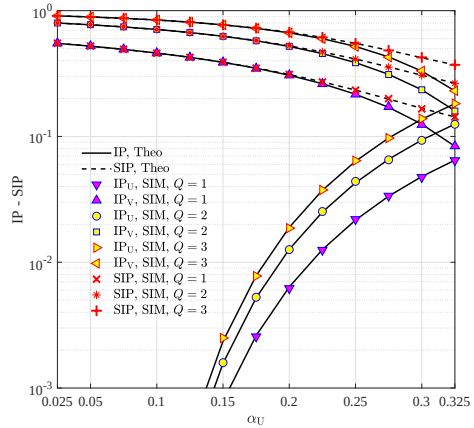

Fig. 5.6: SOP versus α_U with $\Delta = 18$ dB, $L = 4$, $N = 4$, and $M = 2$.

.

Fig. 5.7 indicates that jointly optimizing α_U and L reduces the gap between OP/IP and SOP/SIP, enabling a balanced trade-off between reliability and security.

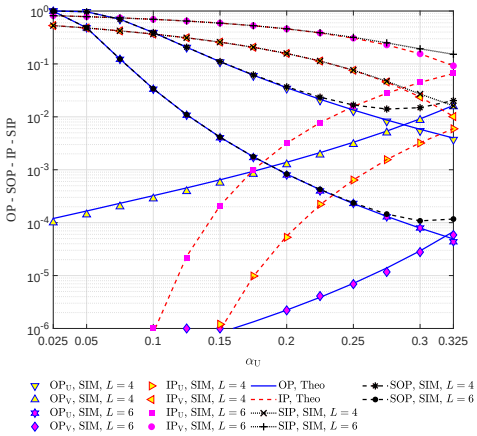

Fig. 5.7: OP, IP, SOP, and SIP versus α_{U} with $\Delta = 16$ dB, $N = 4$, $M = 3$.

5.5. Conclusion

This chapter proposes and analyzes a PLS–HSTRN model integrating RIS with NOMA, FC, and PRS in a multi-cluster eavesdropping scenario, demonstrating simultaneous improvements in reliability and security over benchmark models. Closed-form expressions for OP, SOP, IP, and SIP are derived and validated. The results highlight key trade-offs: increasing L provides gain but raises interception risk; increasing $H_{\max}$ improves decoding but increases latency and degrades security; while NOMA power allocation combined with PRS–RIS enables flexible performance control. Optimal configurations are also identified to balance system requirements. These findings provide a quantitative foundation for the design and optimization of HSTRNs in scenarios requiring high reliability and security.

Chapter 6: Conclusion and Future Work

6.1. Main Contributions of the Dissertation

1. An HSTRN model employing FC under CCI is proposed and analyzed, suitable for high-density and spectrum reuse scenarios. The packet accumulation mechanism significantly improves performance over conventional schemes. Closed-form expressions for OP and SOP are derived and validated via simulations, and a resource optimization problem is formulated to minimize SOP.

2. The model is extended to a multi-cluster scenario integrating NOMA, PRS, and FC in the presence of eavesdroppers. Performance is improved through enhanced spectral efficiency, diversity gain, and FC adaptability. The derived OP, SOP, IP, and SIP expressions enable quantitative evaluation, clarify the reliability–security trade-off, and confirm the effectiveness of the integrated techniques.

3. A PLS–NOMA–HSTRN model integrating RIS with FC and PRS is proposed. RIS enables reconfiguration of the propagation environment, enhances channel gain, and controls the received signal. Results show that the number of RIS elements significantly affects performance and further clarify the trade-off among reliability, security, and latency.

4.The theoretical framework of FC-aided HSTRNs is further completed through closed-form expressions, enabling performance evaluation under various parameters such as channel conditions, CCI, power allocation, RIS configuration, relay number, and user scale, thereby providing a quantitative basis for system design and optimization.

6.2. Future Work

Based on the achieved results and the development trends of HSTRNs in the 6G context, several promising research directions are identified as follows.

1. Extension to two-way relay (TWR) models to enhance spectral efficiency and security.

2. Integration of RIS, EH, and CR to improve both spectral and energy efficiency.

3. Development of advanced security mechanisms based on cooperative jamming (CJ) combined with EH.

4. Consideration of practical conditions such as imperfect SIC/CSI and generalized channel models, along with advanced architectures such as STAR-RIS.

5. Application of RSMA and machine learning for resource optimization and adaptive system control.

These directions contribute to further strengthening the theoretical foundation and guiding practical deployment of HSTRNs, where some initial results have been obtained and reported in [J_3].

LIST OF PUBLICATIONS

J_1. Nguyen Van Toan, Tran Trung Duy, Pham Ngoc Son, Pham Viet Tuan and Tu Lam Thanh, "Security-Reliability Analysis of NOMA-Assisted Hybrid Satellite-Terrestrial Relay Multi-Cast Transmission Networks Using Fountain Codes and Partial Relay Selection with Presence of Multiple Eavesdroppers," *EAI Endorsed Transactions on Industrial Networks and Intelligent Systems*, vol. 12, no. 3, Apr. 2025. DOI: 10.4108/eetinis.v12i3.8604, (Q3, Scopus).

J_2. Nguyễn Văn Toàn, Phạm Ngọc Sơn, Tran Trần Trung Duy, Từ Lâm Thanh và Tạ Văn Thành, "Đánh giá hiệu năng của mạng chuyển tiếp lai ghép vệ tinh–trạm mặt đất sử dụng mã Fountain, NOMA và RIS," *Tạp chí hội Điện tử và Vô tuyến Việt Nam về Điện tử và Truyền thông (REV)*, tập 15, số 3, Jul.–Sep. 2025. DOI: 10.21553/rev-jec.415 (Tạp chí trong nước).

J_3. Nguyen Van Toan, Nguyen Thi Hau, Pham Minh Nam, Pham Ngoc Son and Tran Trung Duy, "Analysis of Security–Reliability Tradeoff of Two-Way Hybrid Satellite–Terrestrial Relay Schemes Using Fountain Codes, Successive Interference Cancelation, Digital Network Coding, Partial Relay Selection, and Cooperative Jamming," *Telecom*, vol. 7, no. 1, Art. no. 5, 2026. DOI: 10.3390/telecom7010005 (ESCI, Scopus, Q_2).

C_1. Nguyen Van Toan, Tran Trung Duy, Pham Ngoc Son, Dang The Hung, Nguyen Quang Sang and Tu Lam Thanh, "Outage Performance Of Hybrid Satellite-Terrestrial Relaying Networks With Rateless Codes In Co-Channel Interference Environment," in *2023 International Conference on System Science and Engineering*, Ho Chi Minh, Vietnam, pp. 468–473, Jul. 2023. DOI:10.1109/ICSSE58758.2023.10227228.

C_2. Nguyen Van Toan, Nguyen Van Hien, Pham Xuan Minh and Pham Ngoc Son, "Performance Evaluation of Hybrid Satellite-Terrestrial Relaying Broadcast Networks Using Fountain Codes and NOMA," in *2024 IEEE International Conference on Consumer Electronics-Asia (ICCE-Asia)*, Danang, Vietnam, pp. 1–4, Jul. 2024. DOI: 10.1109/ICCE-Asia63397.2024.10773917